

DISPERSION-DRIVEN LEWIS ACIDITY OF Cu–SiO₂ CATALYSTS

Giovanni Pampararo^{1*a}, Nicola Scotti^{2*a}, Federica Zaccheria², Nicoletta Ravasio², Damien P. Debecker¹

* Giovanni.Pampararo@uclouvain.be, nicola.scotti@scitec.cnr.it

1. Université catholique de Louvain (UCLouvain), Institute of Condensed Matter and Nanosciences (IMCN), Place Louis Pasteur 1, Louvain-la-Neuve, 1348, Belgium
2. Istituto di Scienze e Tecnologie Chimiche “Giulio Natta” – Consiglio Nazionale delle Ricerche (CNR-SCITEC), Via C. Golgi 19, Milano 20133, Italy

^a-*Giovanni Pampararo and Nicola Scotti equally contribute to this work as first authors.*

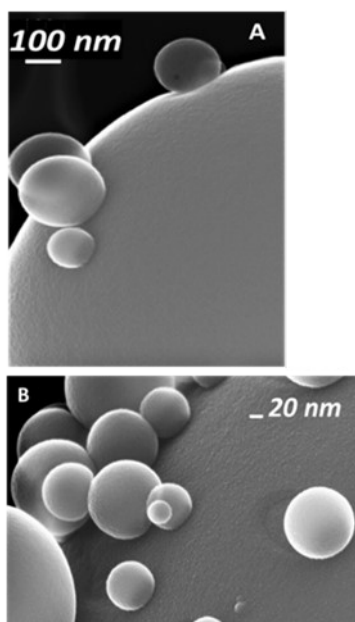


Figure S1: Panels A, B (Secondary electrons imaging) C (backscattered electrons imaging) refer to FE-SEM micrographs acquired on the pristine silica made by AASG method. (Images are taken from ChemicalEngineeringJournal465(2023)142715- ESI)

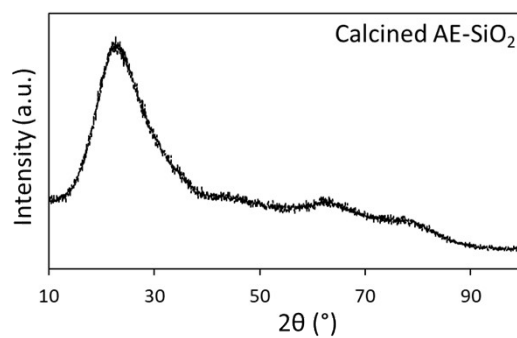


Figure S2: XRD pattern of calcined AE-SiO₂.

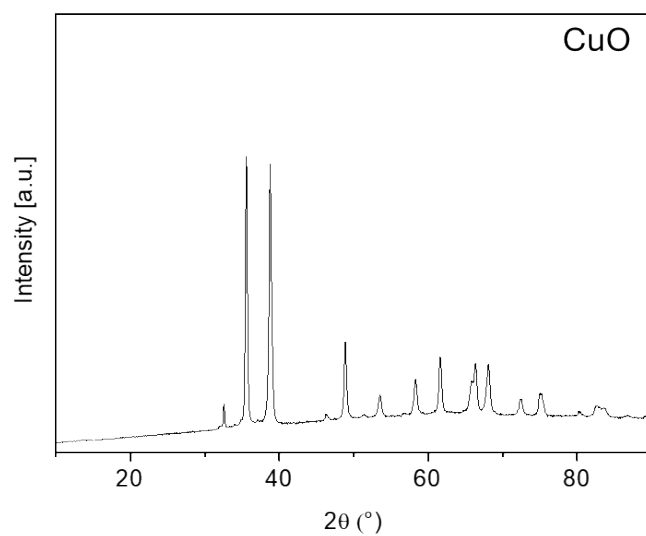


Figure S3: XRD pattern of reference CuO powder.

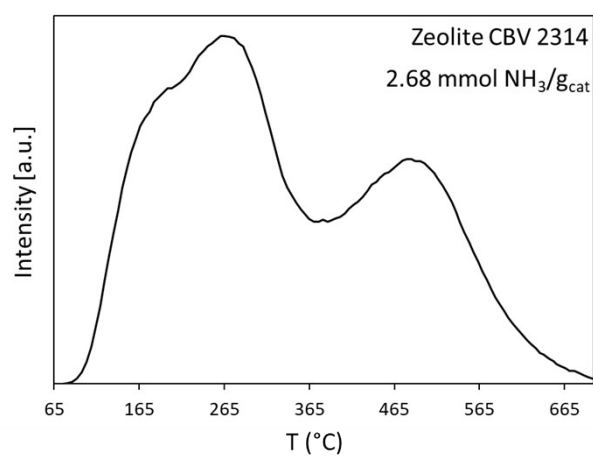


Figure S4: NH_3 TPD acquired over a Zeolite CBV 2314, in the same conditions as for the other catalysts. Relative quantification is reported in the figure. Si/Al mole ratio = 23.

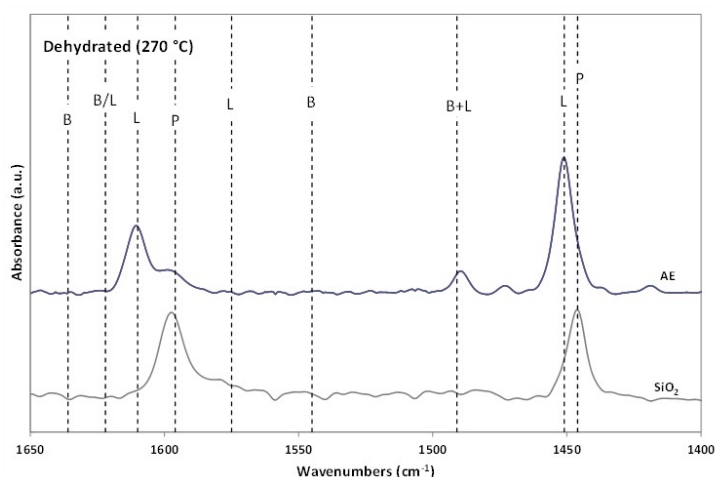


Figure S5: FT-IR of adsorbed pyridine after desorption at 250 °C for AE (oxide form) and SiO₂ samples

To determine the amount of pyridine adsorbed on the Lewis acid sites ($\text{mmol}_{\text{Py}}/\text{g}_{\text{cat}}$), the integration of the band at 1450 cm^{-1} is required [Emeis, C. A. J. Catal. 1993, 141, 347–354].

Here, however, this value is overestimated due its overlap with the band attributed to the trapped pyridine. To mitigate this contribution and to obtain a more accurate assessment of the Lewis acidity, the broad 1450 cm^{-1} signal was deconvoluted into two components (see an example in Figure S6). The component at lower wavenumbers (at about 1446 cm^{-1}) was assigned to trapped pyridine and thus excluded, while the component at higher wavenumber (at about 1450 cm^{-1}) was used for the calculation of Lewis acid sites.

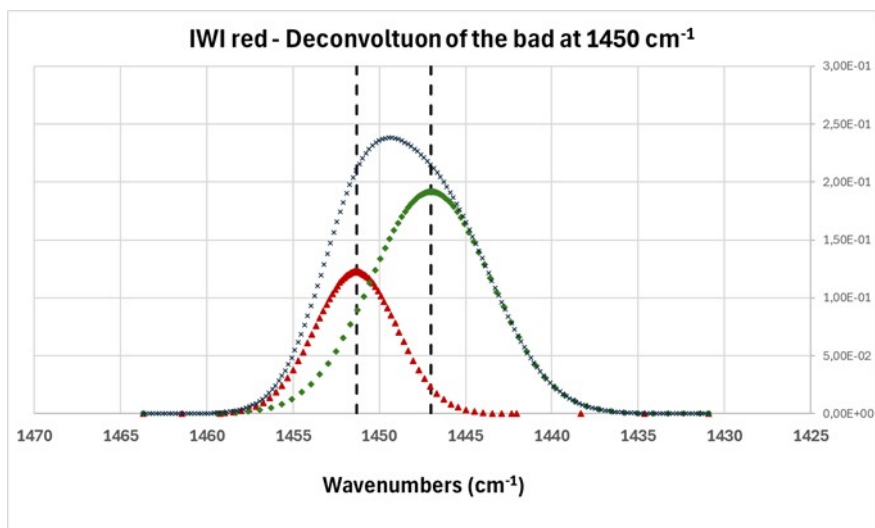


Figure S6: Example of a deconvolution of the band around 1450 cm⁻¹ (IWI red)

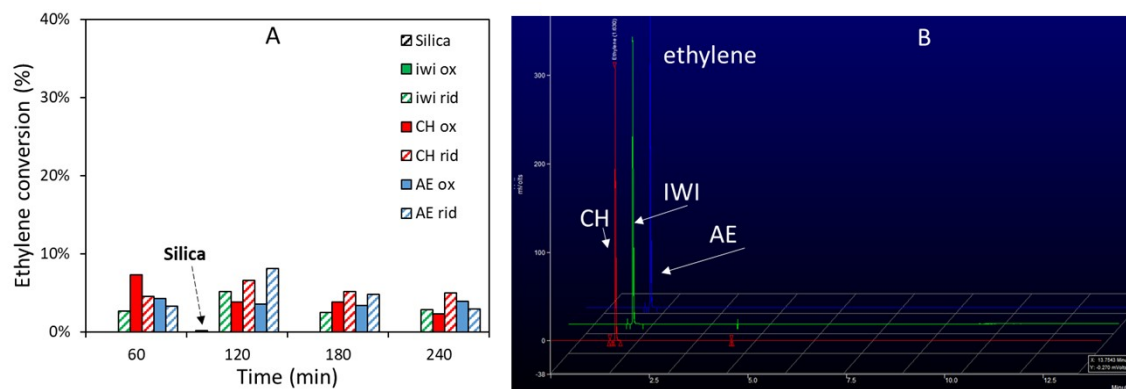


Figure S7: Panel A shows the ethylene conversion upon time of test, panel B show typical chromatogram acquired, where only ethylene is detected all along the duration of the experiments.

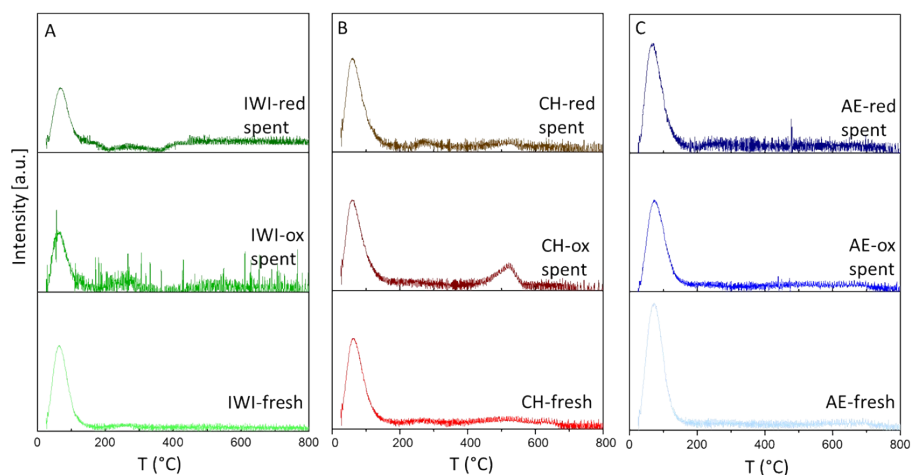


Figure S8: DTGA curves for both fresh and tested catalysts.

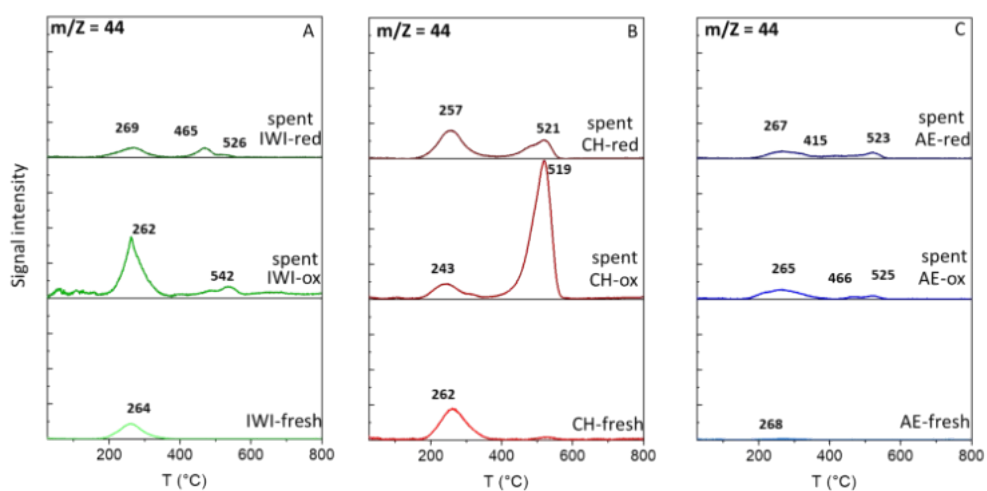


Figure S9: $m/Z=44$ (CO_2) profiles for fresh (not tested) and spent catalysts after ethylene tests (in the oxide form (ox) and reduced form (red) for IWI catalysts (A), CH catalysts (B) and AE catalysts (C). The present measurements are reported in absolute intensity because they are used solely to compare the temperatures at which the peaks occur, and not for quantitative analysis. Quantification is not appropriate here due to variability in detector response across different experiments.

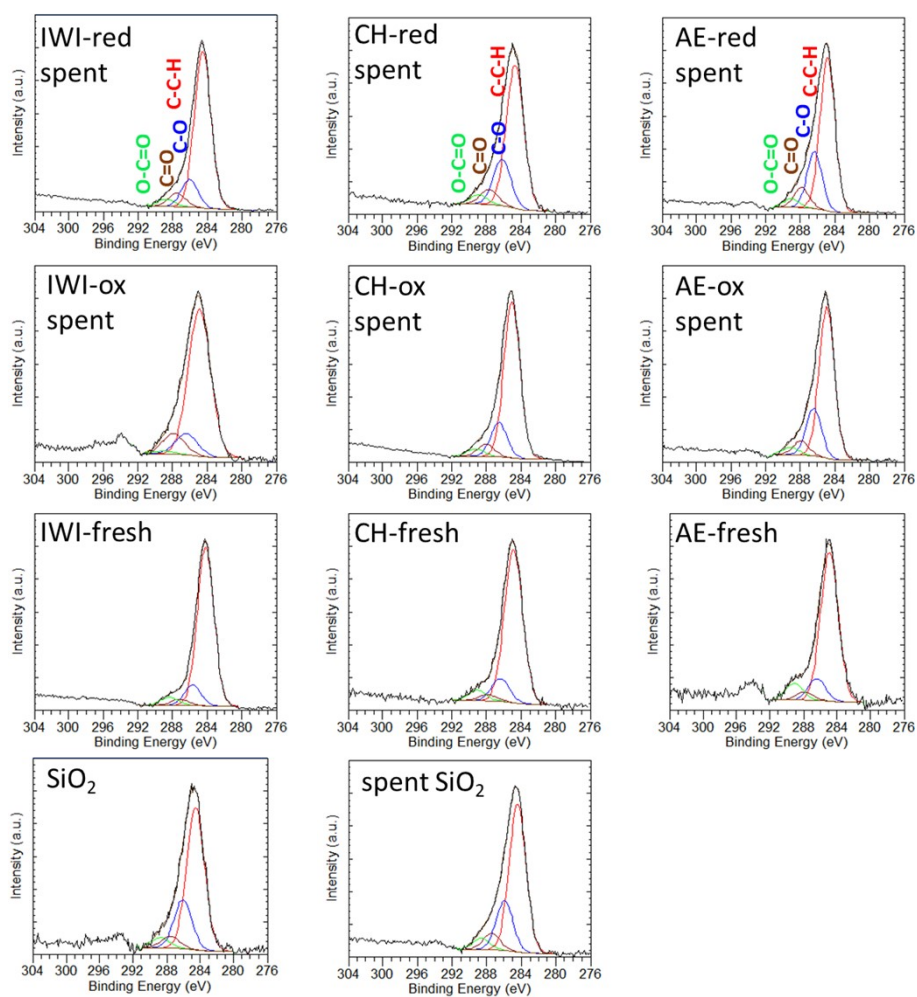


Figure S10: High resolution XPS spectra of C1s region over the fresh and tested catalysts.

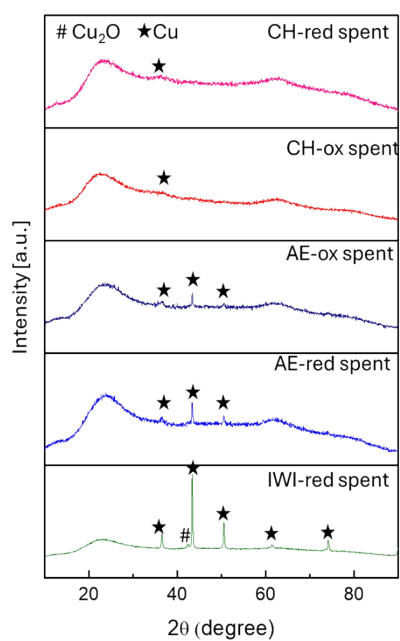


Figure S12: XRD patterns of spent catalysts after ethylene oligomerization experiments. The Crystal size of IWI-red spent is 39 nm while AE-red spent and Ae-ox spent revealed a crystal size of 41 nm and 40 nm. It must be noted that on the reduced catalysts a partial reoxidation to Cu_2O occurred.

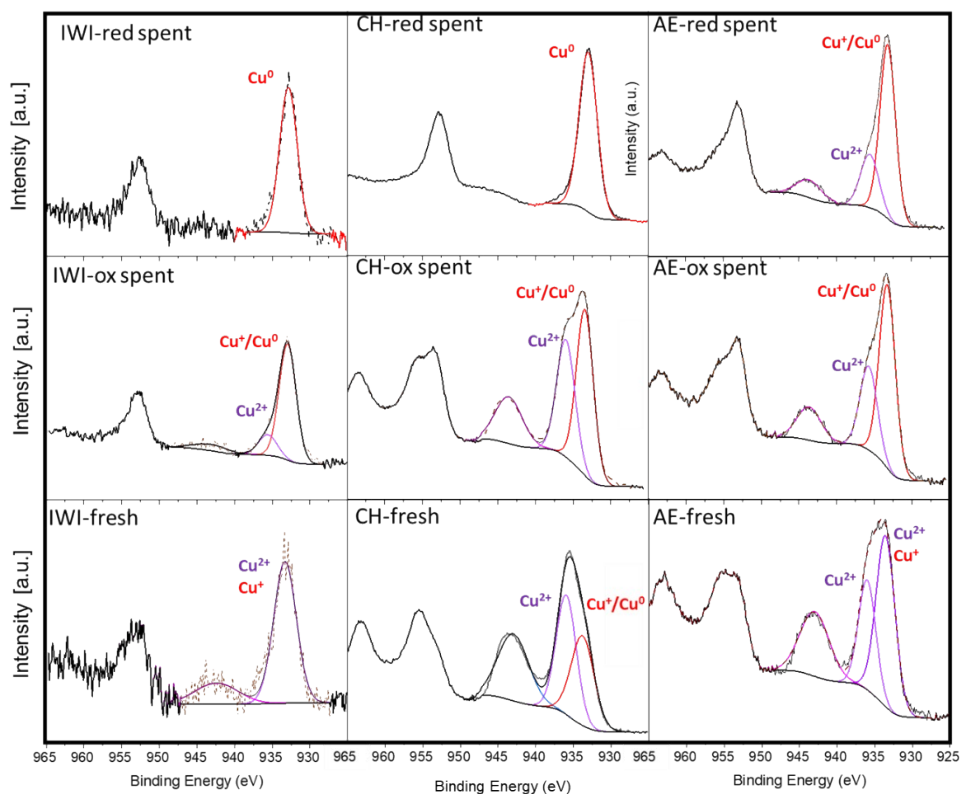


Figure S13: High resolution spectra of Cu 2p region over the fresh and tested catalysts.

Considering the fresh catalyst Cu_{2p} high resolution spectra, the $\text{Cu } 2p_{3/2}$ and $\text{Cu } 2p_{1/2}$ peaks were observed at approximately 933.3 eV and 952.5 eV, respectively, accompanied by shake-up satellite peaks around 943 eV and 963 eV. This confirms the almost exclusive presence of CuO (Cu^{2+} with a d^9 electron configuration). However, over IWI the weak intensity of the satellite peak at 943 eV envisaged a contribution of Cu^+ species to the main peak at 933 eV. On CH fresh, the asymmetry of the main peak, with a clear shoulder at lower binding energy suggested the concomitant presence of partially or totally reduced species i.e. Cu^+/Cu^0 . In the end, on AE fresh, the asymmetry of the Cu_{2p} signals, and the deconvolution of the $\text{Cu } 2p_{3/2}$ peak, reveals two distinct contributions, indicating the presence of i) two Cu^{2+} species with different chemical environments on the catalyst's surface, as previously reported for catalysts prepared by AASG technique or ii) partially reduced species based on Cu^+ .

Focusing on the spent catalysts (-ox), over IWI, the $\text{Cu } 2p_{3/2}$ region revealed a clear peak at 932–933 eV ($\text{Cu } 2p_{3/2}$ orbitals) with a weak satellite peak at 943 eV, meaning that most of the Cu species were reduced Cu^+ and/or Cu^0 . However, the tail at 935–936 eV was assigned to residual Cu^{2+} species. On CH-ox and AE ox a similar interpretation followed, even if the presence of Cu^{2+} species was clearly more important, because of the more intense satellite peaks at 943 eV

and of the two clear features at 933-934 eV. On spent reduced catalysts, for IWI and CH the absence of the satellite and the almost perfect symmetry of the peak at 933 eV were attributed to the fact that almost the totality of copper species is based on Cu⁰. On the contrary, over AE-red the presence of the satellite peak at 943 eV and of the two clear features at 933-934 eV suggested that oxidized residual Cu²⁺/Cu⁺ species were still present at the surface.